International Journal of Recent Technology and Engineering (IJRTE)
ISSN: 2277-3878 (Online), Volume-8 Issue-2, July 2019

Exploration of Hybrid Materials for a Propeller Shaft in Aerospace Applications

Shivanand, Shravankumar B. Kerur

***Abstract:** This paper is a comprehensive analysis of the different composite materials that can withstand the maximum load to be used in shaft instead of the conventional steel which is currently in use. The research focuses on developing a laminated composite propeller shaft for a two-seater aircraft that can withstand maximum load with least deflection. The mathematical model for the shaft of the two-seater aircraft is developed using classical laminate theory. The in-plane forces concerning the applied torque, the strain and stress relations are evaluated for the laminated shaft which is exposed to the in-plane forces. The code is developed in Matlab for the analysis. The results obtained from the Matlab are analysed and the analysis determines that the hybrid material consisting of low carbon steel, epoxy, S glass and T700 fibres is the best suitable for the propeller shaft to withstand maximum load with the least deflection. The orientation angle is considered to be 45 degrees.*

***Keywords:** composite material, classical laminate theory, fibre orientation, propeller shaft, epoxy*

I. INTRODUCTION

In recent times composite material shafts have become the most sought-after option to replace the conventional shafts made of metal in many applications like aircraft, centrifugal separators, helicopters (Chang et al., 2004); (Sino et al., 2008). Generally, the composite structures are analysed through the numerical method with the help of fast development feature of personal computers. The two crucial parameters analysed are geometric and mechanical properties (Araujo et al., 1998). Composite material are characterised by many attractive features such as fire resistant, lightweight, economical and a high ratio of strength and weight when compared to metals making them an alluring option for rotating systems. Furthermore, it was noticed that these materials provide the appropriate behaviours by varying the sequence of the layers with respect to the number, orientation and material of various layers. Hence it is necessary to have an accurately predicted model of dynamic rotor shaft characteristics which is significant for the designing of rotating machines (Yuan et al.,2017). In addition, these researches were found to focus on determining the natural frequencies, critical speeds, unbalance responses and instability thresholds.

Revised Manuscript Received on 30 July 2019.
***** Correspondence Author
Shivanand*, Mechanical Engineering Department, Basaveshwara Engineering College, Bagalkot, Karnataka, India.
Dr. Shravankumar B. Kerur, Mechanical Engineering Department, Basaveshwara Engineering College, Bagalkot, Karnataka, India

Moreover, several finite element formulations were performed for the dynamic analysis of a rotating composite shaft. These research works were usually based on homogenised beam theory and reduced from shell theory (Harursampath et al.,2017). The primary structural functions of a system are the strength, fracture, energy absorption, ductility, thermal stability, energy absorption, stiffness, fracture stiffness, fatigue strength. Recent studies have found that structural weight is not just a function but is a significant part of the design consideration that drives more designs towards lightweight composite materials (Treviso et al.,2015).

This paper concentrates on the analysis of the constituent materials which are used in the laminated composite shafts. The shaft model is developed using classical lamination theory. A code for Matlab is developed, and the outputs obtained are analysed to find the best suitable composite material (which can withstand maximum load) to be used for the propeller shaft of the two-seater aircraft considered for the study.

II. LITERATURE REVIEW

Different studies on composite shafts have shown that there is a maximum reduction of the system weight is achieved by the supercritical operation. Hence the rotordynamicbehaviour is of great importance. Singh, (1992) conducted an analysis of damped vibrations for composite tubes with filament winding using EBMT with Timoshenko shear distribution and SDT. EBMT based rotor dynamics were formulated for a composite rotor that had lumped masses, support bearings.. The LBT was extended to solve the complications of composite rotor dynamics. The author conducted experimental studies for carbon or epoxy shafts wound with filaments at a constant value of wide angles of ± 45 ° and ± 60 °. Bert et al., (1995) conducted a detailed analysis of the dynamic instability for rotating shafts which are subjected to fluctuating torques using different thin shell theories. The study included the effects of both rotation and torsion.

Singh & Gupta (1996) analysed the composite rotor which was supported on eight coefficient bearings which are obtained with the help of equivalent modulus beam theory (EBMT), and layerwise beam theory (LBT). The results of this study were verified for composite as well as metallic rotors. Chen, &Peng, (1998) examined the stability behaviour of the composite shaft which was exposed to loads with axial compression.

EBMT is applied to model the composite shaft with laminations as a Timoshenko shaft. The results of the proposed model matched with the existing models. From the study, it was found that the maximum value of the critical speed of the shaft does not always have to be the ply angle. The ply angle depends on L/R ratio and boundary conditions. There is little effect of the speed on the critical loads of the shaft with thin walls.

Mori-Tanaka mean-field theory was adopted to study the interactions between the finite concentrations in the reinforcement of composite materials (Chang et al., 2004). The existing finite element model was extended to a case which contained fibre by considering the elastic moduli. Whirling speeds in case of rotating shafts and natural frequencies in case of stationary shafts were evaluated using this model. The results proved that orientation of the reinforcements affects the composite shaft characteristics. Alwan et al., (2010) studied and analysed the dynamic behaviour of shafts made of composite materials emphasising on the damping estimation. Carbon/epoxy, glass/epoxy, boron/epoxy were the different materials considered for analysis at various speeds. To determine the composite shafts damping methods like half-power method, force sensors that used hysteresis loop, logarithmic decay curve. A composite drive shaft composed of glass and carbon fibres inside an epoxy matrix was designed with the help of finite element analysis (Talib et al., 2010). The number of layers of carbon-epoxy and glass-epoxy used is 1 and three respectively. The effect of stacking sequence and fibre orientation on the mechanical characteristics and fatigue resistance of the shaft can be understood through the finite element analysis of the proposed model. From the study, it could be inferred that the change in winding angle of the carbon fibres from 0 to 90 resulted in natural shaft frequency to 44.5% and the shift in stacking sequence from best to worst caused a 46.07% of loss in the buckling strength which is a significant concern in the shaft design process.

A parametric study of the stacking sequence on eigenfrequency for the tube shafts was conducted. Khoshravan et al., (2012) presented a design to replace a two-piece steel shaft with a single piece composite drive shaft. The composite driveshaft was made using carbon/epoxy material with high modulus and many layers. The natural frequencies were obtained through modal analysis. Through this model, 72% of weight reduction was achieved in comparison to the conventional model. The results also showed the influence of fibre orientation on the shaft dynamic characteristics.

Fazzolari et al., (2012) presented a model to analyse the free vibrations of composite plates with laminations. The model was designed with the help of higher order shear deformation theory (HSDT). Hamilton's principle is used to derive the boundary conditions and the equations of motion. The shapes of the laminated composite plates are calculated using the Wittrick-Williams algorithm. The proposed method is accurate when compared to the existing methods. Chatelet et al., (2012) proposed a finite element model with two techniques of reduction. In the first technique, the rotating structure is represented as a set of mode shapes concerning the structures at rest and in the second technique structures is represented as identical cyclic structures. The complete system behaviour is acquired through finite element model involving either of the sectors. Gupta, (2015) presented a summary of the research pertaining to the composite shaft dynamics to develop a lightweight rotor system. A composite rotor has a composite shaft whose structure is like that of a tube. The wall thickness has many layers wherein each layer is of different thickness fibre orientation and stacked in a particular sequence. Epoxy is the resin used, and glass or carbon fibres are usually used.

A dynamic analysis for the rotors which were mounted on composite shafts differed from the conventional investigations because of the presence of internal damping in the shaft (Mendonça et al., 2017). Viscoelasticity is a characteristic feature of composite material shafts which can be manufactured using different layers. Simulations of many finite element models are conducted to understand the rotor dynamic behaviour when composite shafts are used. The proposed method required more analysis when compared to conventional rotor analysis because the rotors which have damping shafts had to be assessed for each spin speed of the rotor. Arab et al., (2017) formulated a layerwise shaft theory (LST) for a multi-layered laminated shaft based on finite element method and layerwise displacement. The formulated model considered the influences of fibre orientation, stacking sequence and shear-normal coupling on critical speed and fundamental frequencies. The results of the model proved that it is one of the best alternatives to analyse the dynamic performance of the rotating composite shafts. The results also proved that properties of the materials and the power law index influenced the behaviour of the shafts.

III. RESEARCH METHODOLOGY

Most of the studies focussed on the dynamic analysis of the laminated composite shafts which are utilised in the various application. There are very few studies on the analysis of the constituent materials which are used in the laminated composite shafts. This research aims to determine the best possible composition of the constituent materials to be used in the composite propeller shaft of aircrafts such that it can withstand the maximum loads. The propeller system in an aircraft facilitates its movement through the air. The propeller has two blades or more which are connected by a hub.

The hub attaches the engine shaft and the blades. Figure 1 shows the simple two-seater aircraft considered for the research. Figure 2 illustrates the propeller shaft of the aircraft. Figure 3.shows the components of a propeller shaft of a simple two-seater aircraft. The primary objective of the research is finding a composite material that can withstand maximum load to replace the conventional drive shaft with a laminated drive shaft made of composite material.

Figure 1. Two seater Aircraft
(Source:
https://aircraftengineering.wordpress.com/2011/10/11/aircraft-propellers/)

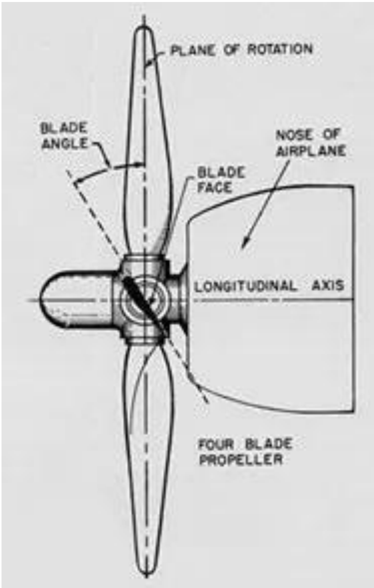

Figure 2. The propeller shaft
(Source:
https://aircraftengineering.wordpress.com/2011/10/11/aircraft-propellers/)

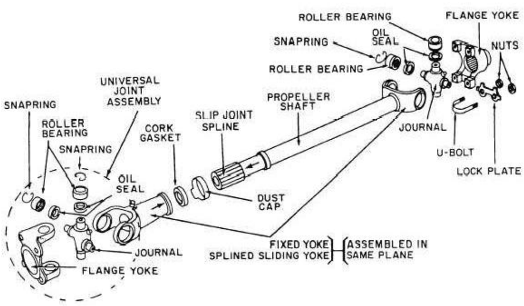

Figure 3. Components of the propeller shaft
(Source:
https://aircraftengineering.wordpress.com/2011/10/11/aircraft-propellers/)

A. Mathematical Modeling

The classical laminate theory is used to model the propeller shaft. The mathematical analysis is presented in this section.

Hooke's law

For an orthotropic material, Hooke's law is given by

$$\{\sigma\} = [Q]\{\varepsilon\} \qquad (1)$$

Where [Q] is a material stiffness matrix. The stress conditions for each layer is given by

$$\begin{Bmatrix}\sigma_{11}\\ \sigma_{22}\\ \sigma_{23}\\ \sigma_{13}\\ \sigma_{12}\end{Bmatrix} = \begin{bmatrix} Q_{11} & Q_{12} & 0 & 0 & 0\\ Q_{12} & Q_{22} & 0 & 0 & 0\\ 0 & 0 & Q_{44} & 0 & 0\\ 0 & 0 & 0 & Q_{55} & 0\\ 0 & 0 & 0 & 0 & Q_{66}\end{bmatrix}\begin{Bmatrix}\varepsilon_{11}\\ \varepsilon_{22}\\ \varepsilon_{23}\\ \varepsilon_{13}\\ \varepsilon_{12}\end{Bmatrix} \qquad (2)$$

The elastic constants are given by

$$Q_{11} = \frac{E_1}{1-v_{12}v_{21}},\; Q_{12} = \frac{v_{12}E_2}{1-v_{12}v_{21}},\; Q_{22} = \frac{E_2}{1-v_{12}v_{21}},\; Q_{44} = G_{23},\; Q_{55} = G_{13},\; Q_{66} = G_{12}$$

Where $E_1, E_2, G_{12}, G_{23}, G_{13}, \wedge\, v_{12}$ are the nth lamina parameters which are obtained using the rule of mixtures. Stress-strain relation of each lamina is given by

$$\begin{Bmatrix}\sigma_{xx}\\ \sigma_{yy}\\ \tau_{yz}\\ \tau_{xz}\\ \tau_{xy}\end{Bmatrix} = \begin{bmatrix} \overline{Q}_{11} & \overline{Q}_{12} & 0 & 0 & \overline{Q}_{16}\\ \overline{Q}_{21} & \overline{Q}_{22} & 0 & 0 & \overline{Q}_{26}\\ 0 & 0 & \overline{Q}_{44} & \overline{Q}_{45} & 0\\ 0 & 0 & \overline{Q}_{45} & \overline{Q}_{55} & 0\\ \overline{Q}_{16} & \overline{Q}_{26} & 0 & 0 & \overline{Q}_{66}\end{bmatrix}\begin{Bmatrix}\varepsilon_{xx}\\ \varepsilon_{yy}\\ \gamma_{yz}\\ \gamma_{xz}\\ \gamma_{xy}\end{Bmatrix} \qquad (3)$$

The stiffness terms which is transformed and reduced is given by

$$\left[\overline{Q}\right] = [T]^{-1}[Q][T]^{-1} \qquad (4)$$

Where

$$[T] = \begin{bmatrix} c^2 & s^2 & -2cs\\ s^2 & c^2 & 2cs\\ cs & -cs & (c^2 - s^2)\end{bmatrix}$$

With c = cos(ϕ), s = sin(ϕ) where □ is the fibre orientation angle of the kth lamina for x-axis beam.

Force moment relations:

A laminate is a fibre reinforced composite material which consists of many layers. Each of the layers will be thin with different orientations. Any two laminates can have an equal quantity of layers, and the fibre angles can also be the same, but the layer arrangement is different.

Figure 4 is the representation of the laminate with N layers. From the figure

h- laminate thickness

h_k- the thickness of the kth layer

z- origin of the thickness coordinate (which is present at the midpoint of the laminate geometry plane.)

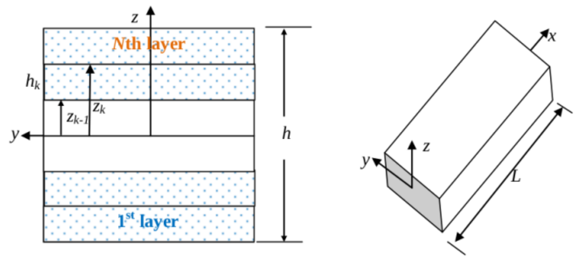

Figure.4 Geometry of the laminate

Laminate is extended in the z-direction from -h/2 to +h/2. Layer 1 is the layer at the most negative location, the next will be layer 2, layer k will be the one at the arbitrary location, and layer N is the one at the most positive z position. The representation of the layer interface locations will be subscripted by z. The first layer is bounded by locations $z_0$and z_1, the second layer by $z_1$and z_2, the kth layer by $z_{k-1}$and z_k, and the Nth layer by $z_{N-1}$and z_N.

Each point inside the volume of the laminate is assumed to be in a state of plain stress. The stress and strain is calculated using strain, curvature and thickness on the reference surface by computing the stiffness matrix of the laminate. Force resultants N_x,

$$\begin{Bmatrix} N_x \\ N_y \\ N_{xy} \end{Bmatrix} = \begin{bmatrix} A_{11} & A_{12} & A_{16} \\ A_{12} & A_{22} & A_{26} \\ A_{16} & A_{26} & A_{66} \end{bmatrix} \begin{Bmatrix} \varepsilon_x^0 \\ \varepsilon_y^0 \\ \gamma_{xy}^0 \end{Bmatrix} + \begin{bmatrix} B_{11} & B_{12} & B_{16} \\ B_{12} & B_{22} & B_{26} \\ B_{16} & B_{26} & B_{66} \end{bmatrix} \begin{Bmatrix} \kappa_x^0 \\ \kappa_y^0 \\ \kappa_{xy}^0 \end{Bmatrix}$$

(5)

N_y, N_{xy} is shown in equation 5 where $\varepsilon^0$and $\kappa^0$are midplane strains and curvatures respectively.

Similarly moment resultants M_x, M_y, $M_{xy}$are represented by the following equation.

$$\begin{Bmatrix} M_x \\ M_y \\ M_{xy} \end{Bmatrix} = \begin{bmatrix} B_{11} & B_{12} & B_{16} \\ B_{12} & B_{22} & B_{26} \\ B_{16} & B_{26} & B_{66} \end{bmatrix} \begin{Bmatrix} \varepsilon_x^0 \\ \varepsilon_y^0 \\ \gamma_{xy}^0 \end{Bmatrix} + \begin{bmatrix} D_{11} & D_{12} & D_{16} \\ D_{12} & D_{22} & D_{26} \\ D_{16} & D_{26} & D_{66} \end{bmatrix} \begin{Bmatrix} \kappa_x^0 \\ \kappa_y^0 \\ \kappa_{xy}^0 \end{Bmatrix}$$

(6)

Where matrix [A], [B] and [D] are

$$A_{ij} = \sum_{k=1}^{N} \left(\underline{Q_{ij}}\right) \quad {}_k z_k - z_{k-1} \qquad (7)$$

$$B_{ij} = \frac{1}{2}\sum_{k=1}^{N} \left(\underline{Q_{ij}}\right) \quad {}_k z_k^2 - z_{k-1}^2$$

(8)

$$C_{ij} = \frac{1}{2}\sum_{k=1}^{N} \left(\underline{Q_{ij}}\right) \quad {}_k z_k^3 - z_{k-1}^3 \qquad (9)$$

The equations are combined as

$$\begin{Bmatrix} N_x \\ N_y \\ N_{xy} \\ M_x \\ M_y \\ M_{xy} \end{Bmatrix} = \begin{bmatrix} [A] & [B] \\ [B] & [D] \end{bmatrix} \begin{Bmatrix} \varepsilon_x^0 \\ \varepsilon_y^0 \\ \gamma_{xy}^0 \\ \kappa_x^0 \\ \kappa_y^0 \\ \kappa_{xy}^0 \end{Bmatrix}$$

(10)

Effective elastic constants

An assumption is made to express the effective material properties in terms of the micromechanical model using mixture rule.

$$E_{11} = V_f E_{11}^f + V_m E_m \qquad (11)$$

$$\frac{1}{E_{22}} = \frac{V_f}{E_{22}^f} + \frac{V_m}{E^m} - V_f V_m \frac{v_f^2 E_m / E_{22}^f + v_m^2 E_{22}^f / E_m - 2 v_f v_m}{V_m E_{22}^f + V_m E_m} \qquad (12)$$

$$\frac{1}{G_{ij}} = \frac{V_f}{G_{ij}^f} + \frac{V_m}{G^m} \text{(ij = 12, 13 and 23)} \qquad (13)$$

$$v_{12} = V_f v_f + V_m v_m \qquad (14)$$

$$\rho = V_f \rho_f + V_m \rho_m \qquad (15)$$

Where E_{11}^f, E_{22}^f, G_{12}^f, G_{13}^f, G_{23}^f, $v_f$and ρ_f are Young's moduli, shear moduli, Poisson's ratio

and mass density, respectively.

The average laminate stresses are defined as

$$\underline{\sigma} = \frac{1}{h}\int_{-h/2}^{h/2} \quad \sigma_x dz \qquad (16)$$

$$\underline{\sigma_y} = \frac{1}{h}\int \quad \sigma_y dz \qquad (17)$$

$$\underline{\tau_{xy}} = \frac{1}{h}\int \quad \tau_{xy} dz \qquad (18)$$

With the help of the relations mentioned above average stress, resultant forces are given by

$$\underline{\sigma_x} \frac{1}{h} N_x \qquad (19)$$

$$\underline{\sigma_x} \frac{1}{h} N_y \qquad (20)$$

$$\underline{\tau_{xy}} = \frac{1}{h} N_{xy} \qquad (21)$$

Therefore the 3x3 laminate matrix is

$$\begin{Bmatrix} \varepsilon_x^0 \\ \varepsilon_y^0 \\ \gamma_{xy}^0 \end{Bmatrix} = \begin{pmatrix} a_{11}h & a_{12}h & 0 \\ a_{21}h & a_{22}h & 0 \\ 0 & 0 & a_{66}h \end{pmatrix} \begin{Bmatrix} \bar{\sigma}_x \\ \bar{\sigma}_y \\ \bar{\tau}_{xy} \end{Bmatrix} \quad (22)$$

The elastic constants obtained from the stress-strain relation are

$$E_x = \frac{1}{a_{11}h} \quad (23)$$

$$E_y = \frac{1}{a_{22}h} \quad (24)$$

$$G_{xy} = \frac{1}{a_{66}h} \quad (25)$$

$$\nu_{xy} = \frac{a_{12}}{a_{11}} \quad (26)$$

$$\nu_{yx} = \frac{a_{12}}{a_{22}} \quad (26)$$

The reciprocity relation between ν_{xy} and ν_{xy} is given by

$$\nu_{xy} = E_x \frac{\nu_{xy}}{E_y} \quad (27)$$

The base material considered for the shaft is a low carbon steel which comprises of 10-18% chromium and 5-8% nickel. This material is the least expensive and has good weldability and machinability properties in comparison with other metals. The composites selected for the research are

- Only low carbon steel
- Only cast iron
- Zirconium + stainless steel
- Cast iron + S glass + T700 fibres
- Low carbon steel + S glass + T700 fibres
- Epoxy + S glass + T700 fibres
- Cast iron + epoxy + S glass + T700 fibres
- Low carbon steel + epoxy + S glass + T700 fibres

Table 1 gives the standard shaft parameters that are considered in the research.

Table 1. Standard shaft parameters

Parameter of shaft	Symbol	Value	Unit
Outer Diameter	d_o	90	mm
Inner Diameter	d_i	83.36	mm
Length of the shaft	L	1250	mm
Thickness of the shaft	T	3.32	mm

IV. RESULTS AND DISCUSSION

The analysis of the materials is done in the following stages.

Stage 1: The first stage involves the analysis of individual plots of load versus deflection for each composite used. These plots give an understanding of the deflections in the materials when different loads are applied.

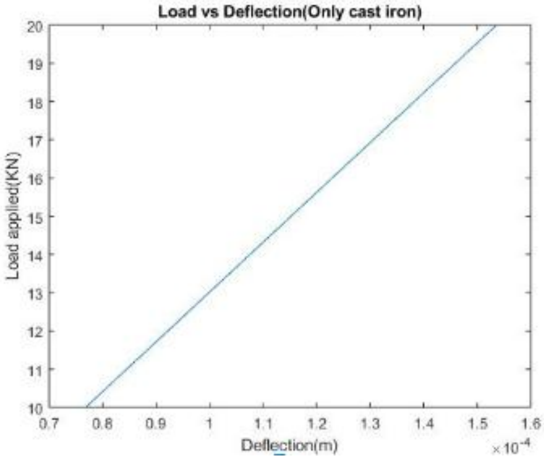

Figure 5. Plot of load vs deflection of cast iron

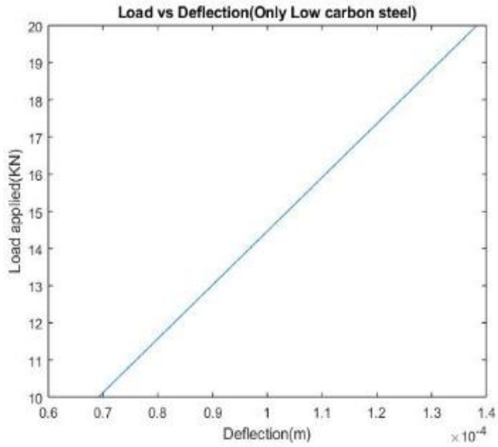

Figure 6. Plot of load vs deflection of low carbon steel

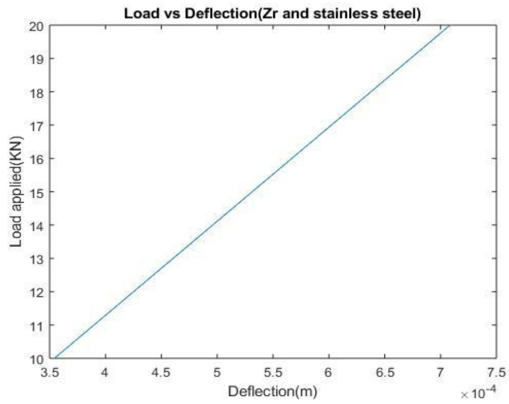

Figure 7. Plot of load vs deflection of Zr& stainless steel

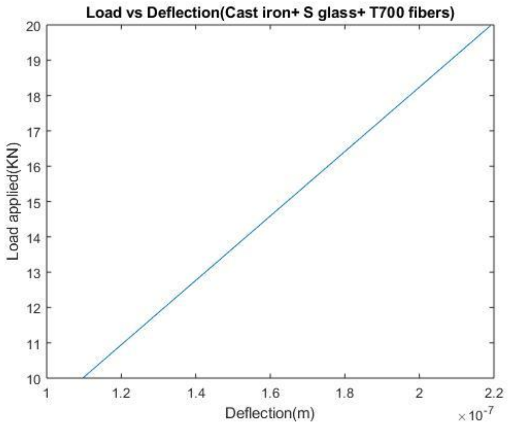

Figure 8. Plot of load vs deflection of cast iron+S glass+T700 fibres

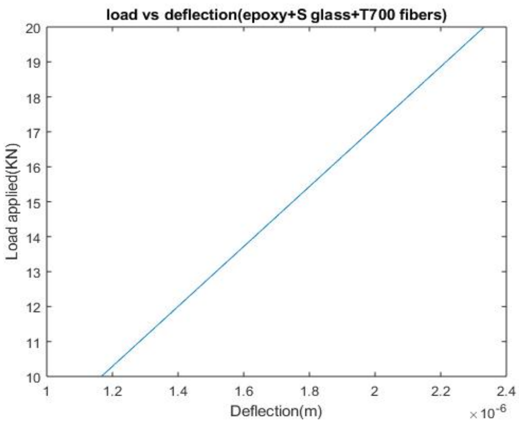

Figure 9. Plot of load vs deflection of epoxy + S glass + T700 fibres

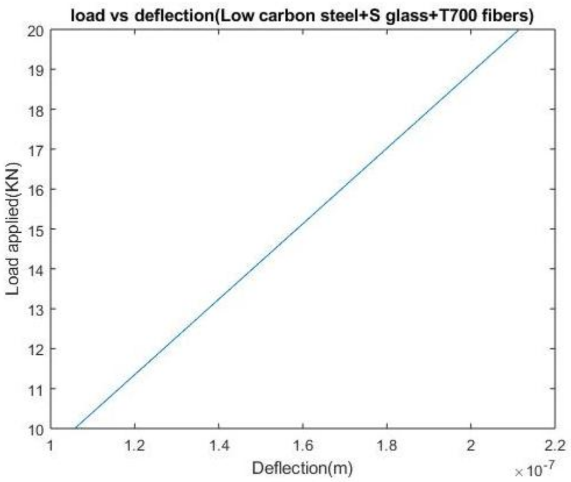

Figure 10. Plot of load vs deflection of ow carbon S glass + T700 fibres

By comparing the plots in figures 7 - 12, it can be inferred that Zr-stainless steel had the maximum deflection which meant that it had a higher fracture point indicating that it is not a feasible option. Low carbon steel + epoxy + S glass + T700 fibres had the least deflection for the applied load hence the lowest fracture point.

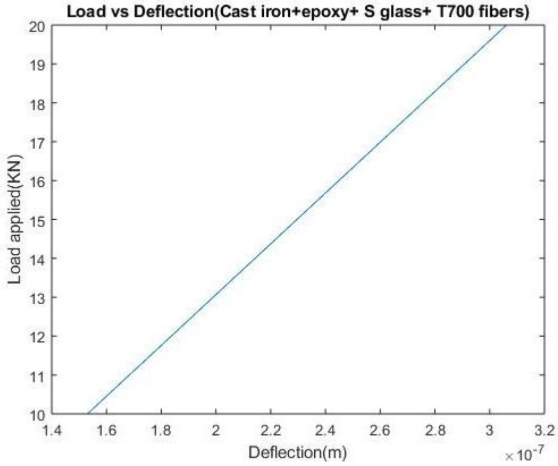

Figure 11. Plot of load vs deflection of cast iron + Epoxy + S glass+T700 fibres

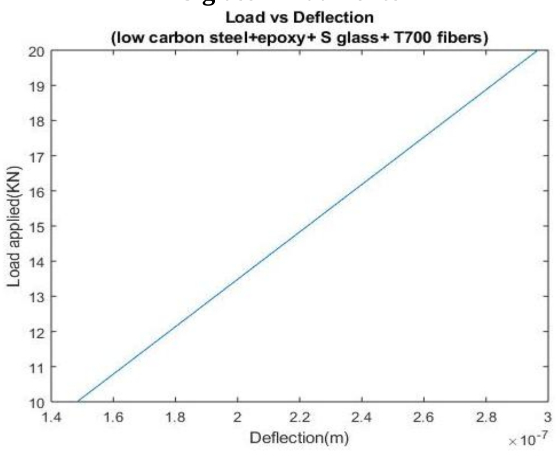

Figure 12. Plot of load vs deflection of low carbon steel + epoxy + S glass+T700 fibres

Stage 2: The next stage involves the plot of torsional load versus the fibre orientation only for the hybrid composites used in the analysis. From the graphs below it can be understood that when the fibre orientation angle is between 30 degrees and 60 degrees the materials can withstand the load.

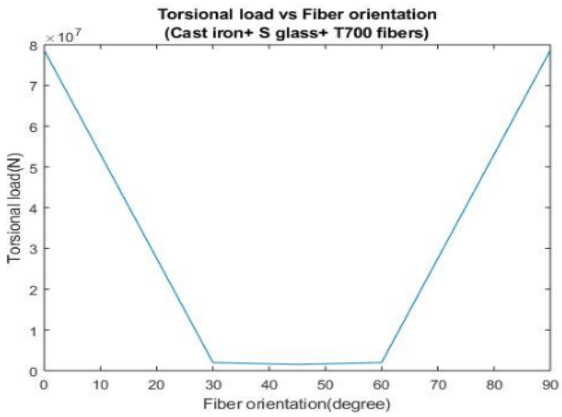

Figure 13. Plot of torsional load vsfibre orientation of cast iron + S glass+T700 fibres

International Journal of Recent Technology and Engineering (IJRTE)
ISSN: 2277-3878 (Online), Volume-8 Issue-2, July 2019

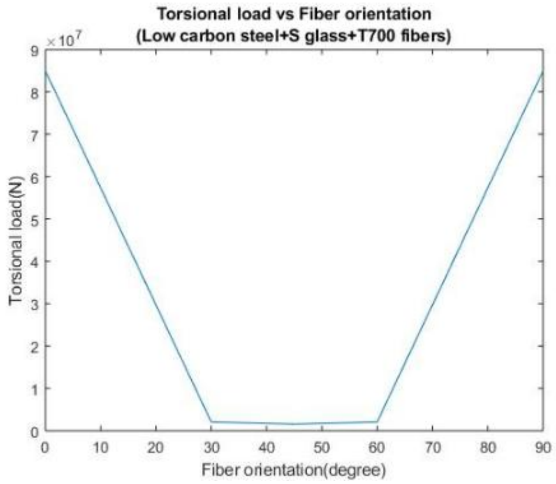

Figure 14. Plot of torsional load vsfibre orientation of low carbon steel + S glass + T700fibres

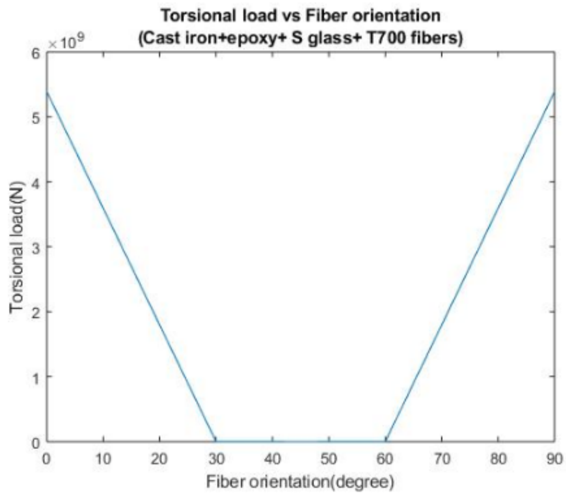

Figure 15. Plot of torsional load vsfibre orientation of cast iron + epoxy + S glass +T700 fibres

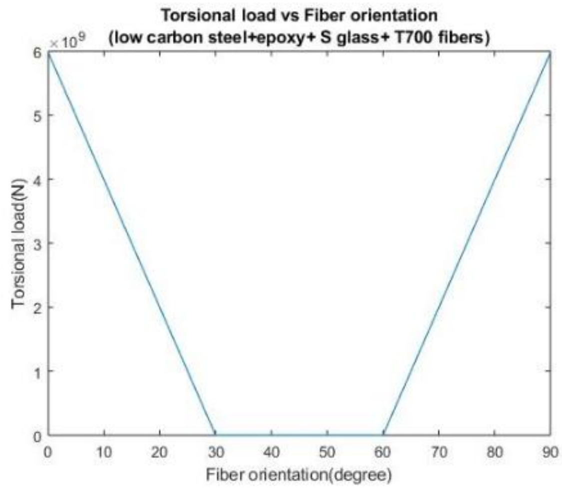

Figure 16. Plot of torsional load vsfibre orientation of low carbon steel + epoxy + S glass + T700 fibres

Stage 3: The final stage involves the plot of Young's modulus versus the fibre orientation of the hybrid materials. From the graphs below an inference can be drawn that young's modulus defined as the ability to withstand changes in length under tension or compression is maximum when the orientation angles of the fibre is 45 degrees.

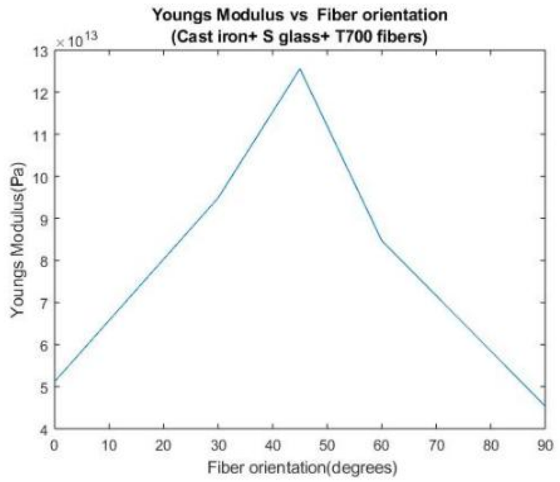

Figure 17. Plot of Young's modulus vsfibre orientation of cast iron + S glass + T700 fibres

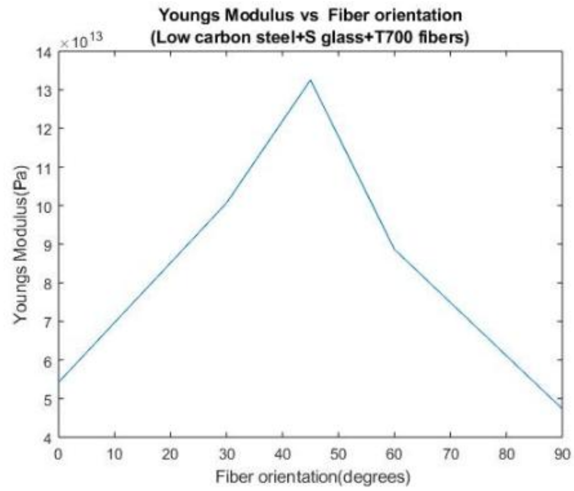

Figure 18. Plot of Young's modulus vsfibre orientation of low carbon steel + S glass + T700 fibres

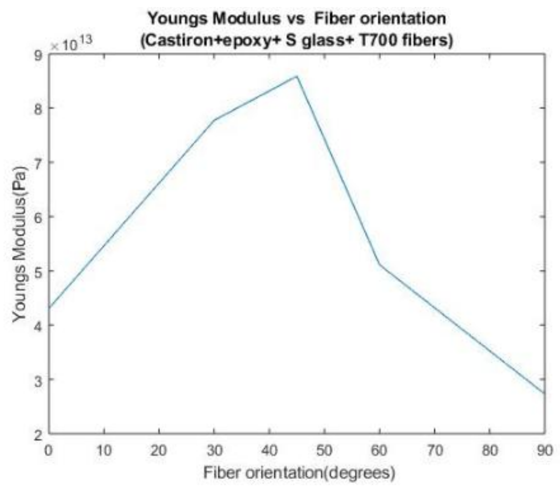

Figure 19. Plot of Young's modulus vsfibreorientation of cast iron + epoxy + S glass + T700

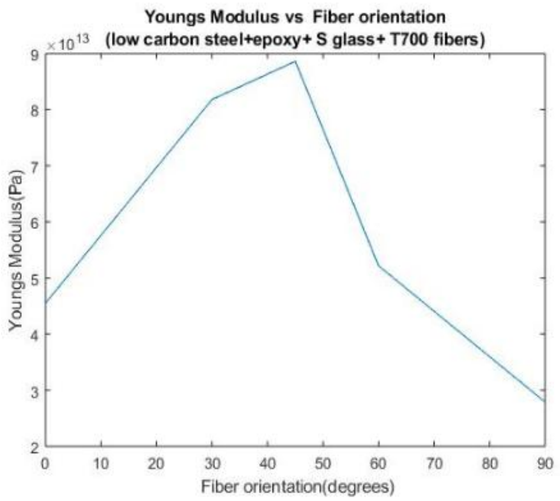

Figure 20. Plot of Young's modulus vsfibre orientation of low carbon steel + epoxy + S glass + T700 fibres

The graphs in figures 21 and 22 give a comparison of the Young's modulus value for the low carbon steel + s glass + T700 fibres, and cast iron + s glass + T700 fibres with and without epoxy.

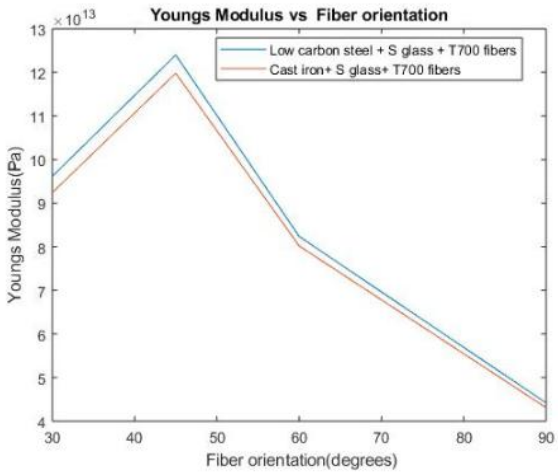

Figure 21. Comparison Plot of Young's modulus vs fiber orientation

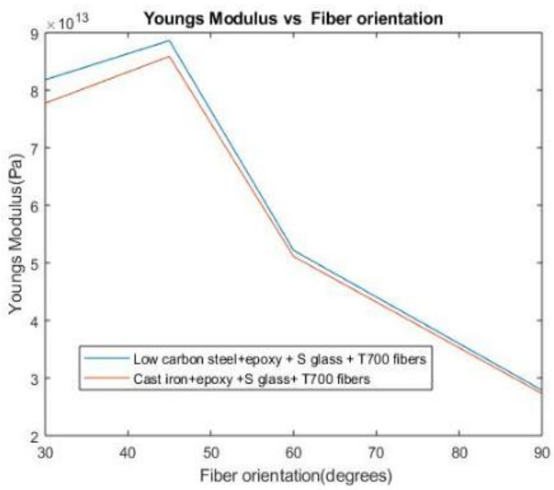

Figure 22. Comparison Plot of Young's modulus vs fiber orientation

Stage 4: Finally the graphs are plotted between the applied load and the deflection caused at different values of the load. Figure 23 gives the comparison plot for Zr-stainless steel, cast iron and low carbon steel from which it can be inferred that for the same maximum value of load Zr-stainless steel had the maximum deflection. Figure 24 gives the comparison plot for load versus deflection for cast iron + S glass + T700 fibres and low carbon steel + S glass + T700 fibres. It shows that cast iron + S glass + T700 fibres has higher deflection when compared to low carbon steel + S glass + T700 fibres which is not feasible because higher the deflection higher will be the fracture point.

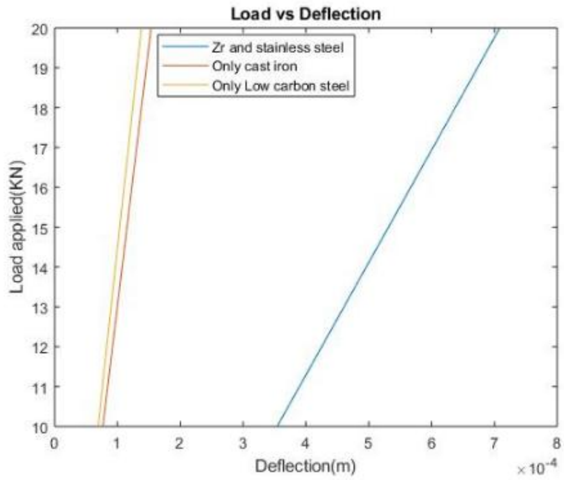

Figure 23. Comparison Plot of load vs deflection

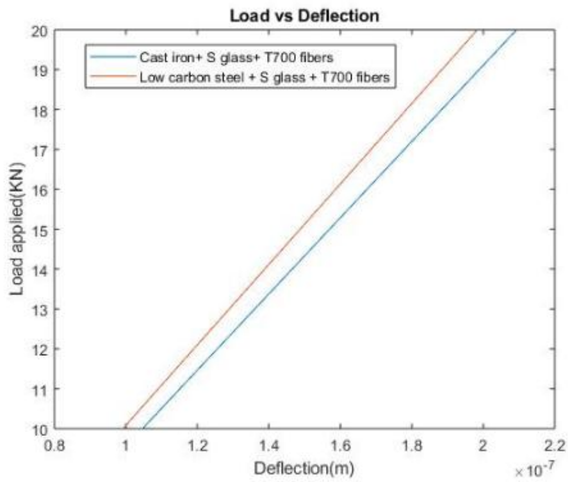

Figure 24. Comparison Plot of load vs deflection

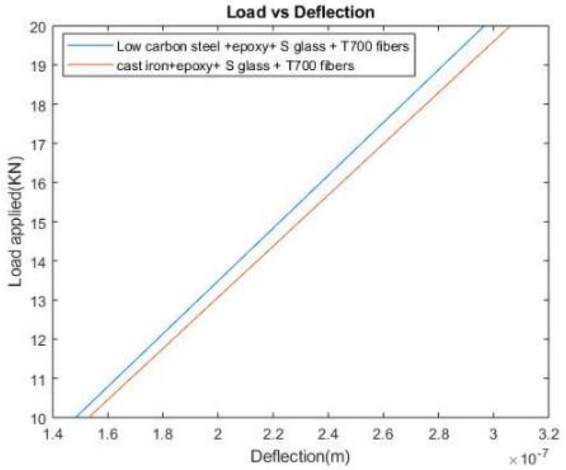

Figure 25. Comparison Plot of load vs deflection

Figure 25 gives the comparison plot for load versus deflection for cast iron + epoxy + S glass + T700 fibres and low carbon steel + epoxy + S glass + T700 fibres. It shows that cast iron + epoxy + S glass + T700 fibres has higher deflection when compared to low carbon steel + epoxy + S glass + T700 fibres.

V. CONCLUSION

This study was conducted to find a suitable composite material for the propeller shaft of an aircraft so that this composite laminated shaft can replace the existing steel shafts. A detailed study was conducted for low carbon steel and cast iron separately and in combination with epoxy, S glass and T700 fibres to analyse their characteristics of orientation angle, young's modulus torsional stiffness, deflection for different values of the applied load. From the analysis it can be concluded that the hybrid composite material that is best suitable for the propeller shaft of the two-seater aircraft is low carbon steel + epoxy + S glass + T700 fibres since it gives minimum deflection, maximum torsional stiffness and the value of its Young's modulus was also minimum. The orientation angle of the fibre was considered as 45 degrees even though the available range was between 30 and 60 degrees since 45 degrees is the only standard value available.

VI. FUTURE SCOPE

In the future, the same hybrid composite model can be analysed in ANSYS software to validate the results obtained from MATLAB. The parameters like maximum torsional deflection, maximum load it can withstand, temperature deflection, the thickness and weight of the component can be determined through analysis in ANSYS software. The interpretation of delamination of the hybrid composite material can also be determined using ANSYS software which was not possible using MATLAB.

REFERENCES

1. Alwan, V., Gupta, A., Sekhar, A. S., &Velmurugan, R. (2010). Dynamic analysis of shafts of composite materials. *Journal of Reinforced Plastics and Composites*, *29*(22), 3364-3379.
2. Araujo, A. L., Soares, C. M., & De Freitas, M. M. (1996). Characterization of material parameters of composite plate specimens using optimization and experimental vibrational data. *Composites Part B: Engineering*, *27*(2), 185-191.
3. Arab, S. B., Rodrigues, J. D., Bouaziz, S., &Haddar, M. (2017). Dynamic analysis of laminated rotors using a layerwise theory. *Composite Structures*.
4. Bert, C. W., & Kim, C. D. (1995). Dynamic instability of composite-material drive shaft subject to fluctuating torque and rotational speed. *Dynamics and Stability of Systems*, *10*(2), 125-147.
5. Chang, C. Y., Chang, M. Y., & Huang, J. H. (2004). Vibration analysis of rotating composite shafts containing randomly oriented reinforcements. *Composite structures*, *63*(1), 21-32.
6. Chang, M. Y., Chen, J. K., & Chang, C. Y. (2004). A simple spinning laminated composite shaft model. *International journal of solids and structures*, *41*(3-4), 637-662.
7. Chatelet, E., Lornage, D., &Jacquet-Richardet, G. (2002). A three-dimensional modelling of the dynamic behaviour of composite rotors. *International Journal of Rotating Machinery*, *8*(3), 185-192.
8. Chen, L. W., &Peng, W. K. (1998). The stability behaviour of rotating composite shafts under axial compressive loads. *Composite Structures*, *41*(3-4), 253-263.
9. Fazzolari, F., Boscolo, M., & Banerjee, J. (2012). Dynamic Stiffness Formulation and Free Vibration Analysis of Composite Plate Assemblies using Higher Order Shear Deformation Theory. In *53rd AIAA/ASME/ASCE/AHS/ASC Structures, Structural Dynamics and Materials Conference 20th AIAA/ASME/AHS Adaptive Structures Conference 14th AIAA* (p. 1470).
10. Flower, H. M. (2012). *High performance materials in aerospace*. Springer Science & Business Media.
11. Guadagno, L., Raimondo, M., Vittoria, V., Vertuccio, L., Naddeo, C., Russo, S., ...&Tucci, V. (2014). Development of epoxy mixtures for application in aeronautics and aerospace. *RSC Advances*, *4*(30), 15474-15488.
12. Gubran, H. B. H., & Gupta, K. (2005). The effect of stacking sequence and coupling mechanisms on the natural frequencies of composite shafts. Journal of sound and vibration, 282(1-2), 231-248.
13. Gupta, K. (2015). Composite Shaft Rotor Dynamics: An Overview. In *Vibration Engineering and Technology of Machinery* (pp. 79-94). Springer, Cham.
14. Harursampath, D., Harish, A. B., & Hodges, D. H. (2017). Model reduction in thin-walled open-section composite beams using variational asymptotic method. Part I: Theory. Thin-Walled Structures.
15. Jin, F. L., Li, X., & Park, S. J. (2015). Synthesis and application of epoxy resins: A review. *Journal of Industrial and Engineering Chemistry*, *29*, 1-11.
16. Khoshravan, M. R., &Paykani, A. (2012). Design of a composite drive shaft and its coupling for automotive application. *Journal of applied research and technology*, *10*(6), 826-834
17. Lubin, G. (2013). *Handbook of composites*. Springer Science & Business Media.
18. Mangalgiri, P. D. (1999). Composite materials for aerospace applications. *Bulletin of Materials Science*, *22*(3), 657-664.
19. Mendonça, W. R. D. P., De Medeiros, E. C., Pereira, A. L. R., & Mathias, M. H. (2017). The dynamic analysis of rotors mounted on composite shafts with internal damping. *Composite Structures*, *167*, 50-62.
20. Na, S., Yoon, H., &Librescu, L. (2006). Effect of taper ratio on vibration and stability of a composite thin-walled spinning shaft. *Thin-walled structures*, *44*(3), 362-371.

21. Shanyi, D. U. (2007). Advanced composite materials and aerospace engineering [J]. *ActaMateriaeCompositaeSinica*, *1*, 000.
22. Singh, S. P. (1992). *Some studies on dynamics of composite shafts* (Doctoral dissertation).
23. Singh, S. P., Gubran, H. B. H., & Gupta, K. (1997). Developments in dynamics of composite material shafts. *International Journal of Rotating Machinery*, *3*(3), 189-198.
24. Singh, S. P., & Gupta, K. (1996). Composite shaft rotordynamic analysis using a layerwise theory. *Journal of Sound and Vibration*, *191*(5), 739-756.
25. Sino, R., Baranger, T. N., Chatelet, E., &Jacquet, G. (2008). Dynamic analysis of a rotating composite shaft. *Composites Science and Technology*, *68*(2), 337-345.
26. Source: https://aircraftengineering.wordpress.com/2011/10/11/aircraft-propellers/
27. Talib, A. A., Ali, A., Badie, M. A., Lah, N. A. C., &Golestaneh, A. F. (2010). Developing a hybrid, carbon/glass fibre-reinforced, epoxy composite automotive drive shaft. *Materials & Design*, *31*(1), 514-521.
28. Treviso, A., Van Genechten, B., Mundo, D., &Tournour, M. (2015). Damping in composite materials: Properties and models. Composites Part B: Engineering, 78, 144-152.
29. Yuan, Z., Crouch, R., Wollschlager, J., & Fish, J. (2017). Assessment of multiscale designer for fatigue life prediction of advanced composite aircraft structures. Journal of Composite Materials, 51(15), 2131-2141.

AUTHORS PROFIL

Shivanand received AMAeSI(B.E.) from-Aeronautical Society of India New Delhi in 1997, M.Tech. in Mechanical Fluid in 2005, and M.Tech. in Aerospace Engineeringfrom JNTU Hyderabad in 2010. Presently he is working as an Assistant Professor in Government Engineering College Raichur (Karnataka) and deputed to Basaveshwar Engineering College Bagalkot for pursuing full time PhDfrom VTU Belagavi. He has been teaching at graduate level engineering courses since 2006. He also has 15 years of industrial experience in Indian Air Force. His research interests include strength of materials, composite/hybrid materials, Vibration, Fluid and structural Analysis.

Dr. SHRAVANKUMAR B. KERUR received B.E. from B.E.C. Bagalkot ,M.Tech. (Machine Design.)from B.E.C. Bagalkot, received the Doctorate degree from IIT Kharagpur in Applied Mechanics . He started his career as a Lecturer and later on promoted as Associate Professor in 2013. He is presently working as Associate Professor Department of Mechanical Engineering, Basaveshwar Engineering College BAGALKOT. His research area is Strength of Materials, Machine Design, FEA, Composite/Smart Materials, Vibration, and Fluid Structure Interaction.